Conference Paper

Implications for voltage control with increased distributed generation on interconnected power networks

Thwaites, D.P. and Vagapov, Y.

This is a paper presented at the 2021 IEEE Young Researchers in Electrical and Electronic Engineering Conference, Moscow, Russia, 26-29 January 2021.

Implications for Voltage Control with Increased Distributed Generation on Interconnected Power Networks

Daniel P. Thwaites, Yuriy Vagapov
Faculty of Art, Science and Technology
Wrexham Glyndwr University
Wrexham, UK

***Abstract*—Electrical distribution networks in the UK are likely to experience increasing levels of distributed and renewable generation connections in the near future; emphasised by the 2019 government pledge to achieve net-zero carbon emissions by 2050. This paper focuses on a specific group of 33/11kV transformers on a meshed network in the UK and aims to model how the introduction of wind and solar farms on the interconnected 11kV distribution network could affect automatic voltage control devices upstream.**

Keywords—distributed power generation, power system modelling, voltage control, bidirectional power flow, load flow

I. INTRODUCTION

After generators, power transformers are the backbone to the electrical industry allowing for practical generation voltages, long-distance transmission, and workable consumption; however, at every step-up or step-down in voltage power losses are accumulated [1]. The recent European Commission regulations [2], [3], whilst a step in the right direction, do little to address the losses in existing transformers.

Globally there is momentum towards a greener world that captures carbon rather than consumes it. Using fossil fuel power plants to generate electricity is losing favour, and governments are set to encourage widespread uptake of renewable generation at a consumer level, including Wind Farms, Solar Farms, Micro-Grids, etc. The carbon-neutral commitment also introduces prospective increases in typical consumer demand; particularly as domestic and commercial electric vehicle (EV) use becomes more mainstream, and daily battery charging becomes a regularity [1]. The uptake of EV will intensify towards the end of the decade as the UK plans to ban petrol and diesel vehicle sales by 2030 [2]. Small-scale generation technologies are predominately connected at lower voltage levels within the 11kV/415V domain. The power produced by distributed power generation (DG) and how it could affect voltage control upstream on the Scottish Power Manweb (SPM) Network is investigated in this paper.

II. MODELLING METHODOLOGY

The terms Power Flow Analysis (PFA) and Load Flow Analysis (LFA) are interchangeable, but both describe the category of Power Systems Analysis (PSA) that involves the analysis of currents, voltages and bidirectional power flow in a steady-state system. There are other categories of PSA, such as Stability/Contingency and Short Circuit Analysis [3]-[6].

To perform PFA successfully, a method of iterative convergence is employed to compute the voltage magnitude and phase angle at each bus. The power component values of the network must first be known, with which a bus admittance matrix can be created (1). Each bus is assigned an initial voltage estimate, which is updated at each iteration. The buses are updated based on the resultant estimates of the previous iteration; where each bus is updated independently since individual bus voltage is affected by all other bus voltages. With each iteration, the voltage at each bus becomes a value closer to being correct as per the parameters of the computation. This process is repeated until the bus voltages reach a specified tolerance with respect to the correct value and achieve convergence [3], [7].

$$\mathbf{Y}_{BUS} * \mathbf{V}_{BUS} = \mathbf{I}_{BUS} \tag{1}$$

where $\mathbf{Y}_{BUS}$ is the bus admittance matrix; $\mathbf{V}_{BUS}$ is the bus voltage matrix; $\mathbf{I}_{BUS}$ is the matrix of the current injected in each node.

PFA models use a type of node called a bus to connect points of generation, loads, transformers, and transmission lines. Measurement of voltage and current can be taken at these nodes for PFA to establish real and reactive power flow at each bus. Two quantities must be known for each point of generation or load; generally, *PQ* quantities are specified at the load while the voltage (V) and voltage phase angle (δ) are known at the source [7]. There are three types of bus for PFA seen in Table I.

TABLE I. BUS CLASSIFICATIONS AND QUANTITIES.

Bus Type	Known/ Specified Quantities	Unknown Quantities Determined by PFA
Swing, Slack or Reference	V, δ	P, Q
Generator, Voltage Control or *PV*	P, V	Q, δ
Load or *PQ*	P, Q	V, δ

The swing, slack or reference bus is necessary in PFA models to account for power losses in transmission lines. The power balance relationships are:

978-1-6654-0476-1/21/$31.00 ©2021 IEEE

$$P_L = \sum_{i=1}^{N} P_{Gi} - \sum_{i=1}^{N} P_{Di} \quad (2)$$

$$Q_L = \sum_{i=1}^{N} Q_{Gi} - \sum_{i=1}^{N} Q_{Di} \quad (3)$$

where P_L and Q_L are power losses in transmission lines; P_{Gi}, Q_{Gi} are generator power quantities; and P_{Di}, Q_{Di} are demand power quantities [8].

The generator bus describes the type of node that will be required for the introduction of DG at 11kV on the Simulink model. The magnitude of real power (MW) injected into the network can be controlled from this type of node. All 11kV loads on the network are defined as a 'Load Bus' in the model. The real and reactive power quantities are known values and are derived from the Scottish Power Energy Networks load forecast data for the group [1], [8].

The power balance equations (4), (5) relate to the load bus by:

$$P_i + jQ_i = \left(P_{Gi} + P_{Di}\right) + j\left(Q_{Gi} + Q_{Di}\right) \quad (4)$$

where P_D and Q_D are negative quantities, and P_G and Q_G are positive quantities [8].

There are three main methods of PFA:

Gauss-Seidel Method. With respect to mathematical complexity and subsequent programming for digital computation, this method is the simplest of the three available PFA methods. Using this method, there is a direct relationship between the rate of convergence and the size of the system. Hence, the larger the system the more time it takes for the math to converge on a value within the specified tolerance [8].

Fast-Decoupled Power Flow Method. This method relies on the fact that transmission lines have a high reactance/resistance (X/R) ratio, making changes in real power (ΔP) less sensitive through changes in voltage magnitude (ΔV); and more sensitive through changes in voltage phase angle ($\Delta\delta$). Reactive power is affected in an opposite manner, being affected more by voltage magnitude than the phase angle. Hence J2 and J3 of the Jacobian matrix can be set to zero allowing the separation of the matrix equation into two decoupled equations that demand significantly less computation to solve when compared with other methods [8].

Newton-Raphson Method. This method is used by the Simulink Load Flow Tool. The method is capable of reaching convergence with significantly less iterations than the Gauss-Seidel method because the rate of convergence is not linked to the size of the system. The major flaw of this method is the number of mathematical calculations required per iteration. When computed digitally, this method requires more memory, and it is more complex to program the logic when compared with the Gauss-Seidel method [8]. By installing Simulink on a computer with a suitable hardware specification, we overcome these drawbacks and are provided with a PFA tool that allows the user to perform analysis on a large network model with reasonably fast and reliable results [8].

Steps for using the Newton-Raphson algorithm are as follows:

1. Create the bus admittance matrix for the system ($\mathbf{Y}_{BUS}$).
2. Make initial estimations of voltages.
   a. $\delta_i° = 0$ for $i = 1,2,3\ldots N$ (except for swing bus)
   b. $|V_i| = 1.0$ for $i = M+1, M+2\ldots N$ (for PQ busses only)
   c. $|V_i| = |V_i|$ (spec.) (for swing bus only)
3. Calculate the real and reactive power for the load bus.
4. Check Q-limit violation at the swing bus (either act as PV or PQ bus).
5. Compute mismatch vector finding the change in P_i and Q_i compared with spec.
6. Compute P_i and Q_i maximum values.
7. Compute Jacobian Matrix and obtain static correction vector.
8. Update state vector for voltage and voltage phase angle.
9. Repeat until all nodes are within tolerance of the swing bus complex voltages.

III. Modelling Computation

Simulink mathematical modelling software is a visual tool that allows the user to create a model using blocks, nodes and connections. The versatility of the software provides a platform for modelling a wide array of system types. The Load Flow Tool that can be accessed through the powergui block allows the user to initialise a steady state simulation of three-phase networks to perform load flow analysis. The tool uses the Newton-Raphson method to provide a fast convergence solution when compared to alternative methods such as the 'Machine Initialisation tool' that only has simple load flow features.

IV. Model Development

The Simulink model was built following the structure illustrated by the block diagram in Fig. 1. The power flow at 33kV is to be observed; hence, the source for the model is the point where 132kV is transformed to 33kV. The load is specified at 11kV and DG is inserted at this voltage level. In reality, 132kV is delivered from sources of generation via the Transmission Network to the DNO's Grid substations at 132/33kV transformers. 11kV is transformed down to 415V at X and Y type substations for consumers [1].

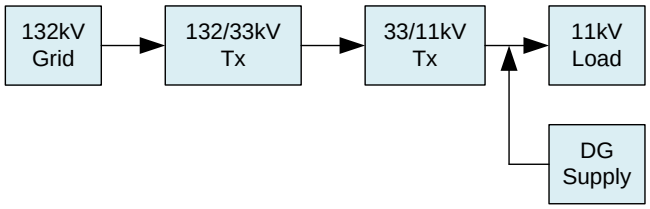

Fig. 1. Top level block diagram of PFA model.

The introduction of wind and solar was used to represent DG in the model. Two 5.25MW wind farms and two 4.0MW solar farms were added at the 11kV interconnected voltage level. Each with a 'Three Phase Source' block and a star-star connection type step-up transformer. A 'Load Flow Bus' node was placed at the location between the step-up transformer and three-phase source blocks for each DG arrangement.

For the wind farms, the values were derived from the information provided on the Scottish Power Renewables webpage, stating that the turbines used at Kilgallioch Windfarm (SP North) are 2.45MW Siemens Gamesa Turbines. Examination of the available turbines from Siemens shows that the closest match is the SG 2.6-114 Siemens Gamesa Onshore Wind Turbine (P_{nom} = 2.625MW). Hence for the case of small sites with two wind turbines, 5.25MW would be the nominal power generated. With reference to the datasheet for the SG 2.6-114 the nominal rms voltage for the turbines is 690V [9], [10].

Examining a relevant case study from the BRE National Solar Centre based in Cornwall, UK; it was determined that each solar panel normally produces approx. 269.1 Watts. Meaning for a 4MW Solar Farm, we would need 14864 panels. It can be assumed that the phase-phase voltage for each panel is approx. 270Vac. Quoting the study "A planning application was subsequently submitted for the development of a 1.55MW 'solar farm' at the site. This would involve the installation of 5,760 solar panels on a site of 3.88ha with associated inverters, substation and security fencing." For a 4MW Solar Farm, this equates to 1.55MW/5760 = 269.1; 4MW/269.1 = 14864 panels. The standard model parameters for a Solar PV from Simulink set the voltage at 260Vac, so we assume that for the selected case from BRE, the wattage per panel was calculated with a nominal current value of 1A. Hence $P = IV = 1 \times 269.1 = 269.1$W. If we set the base current at 270V and keeping the power at 269.1W, then the nominal current would be 0.997A per panel [11].

V. Model Test and Analysis

The schedule of tests was designed to follow 20% increase in DG year on year; with an eventual usage of 80% by 2023/24. Testing at 100% has been carried out for the year 2024/25 with the presumption electric vehicle (EV) uptake will significantly increase network demand through this period. It is however highly unlikely that all LV connected renewables will feed the network at 100% simultaneously.

The active power P_{LF} that flows in reverse to the grid site secondary side (33kV) is summated to provide a value of total active power that the chosen transformer group will feedback to the network in the event of over-generation on the LV DG. Once the test results were recorded, an analysis table was populated with summated values of real and reactive power, indicating the total 33kV load flow. The effects of the simulation were analysed by observing the change in power quantities as levels of DG increase, and by observing the magnitude of change for each test in comparison with baseline *PQ* values. A total of 6 tests were carried out as per Table II.

The load *PQ* values were changed as per the schedule of tests, derived from the forecast level of demand for the transformer group as per the circuit data [1].

The real power values for the DG blocks (Fig.2) were increased incrementally when proceeding through the tests.

TABLE II. MODELLING TEST SCHEDULE.

Test Number	Fo recast Period	Level of DG Exposure
1	2019/20	Baseline
2	2020/21	20%
3	2021/22	40%
4	2022/23	60%
5	2023/24	80%
6	2024/25	100%

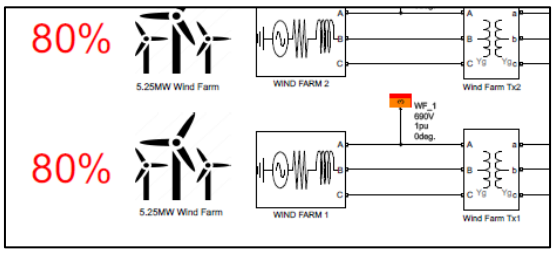

Fig. 2. LFA Model – Wind Farm Generation at interconnected 11kV.

VI. Findings

The rate of change in real power magnitude for power flowing through 'Grid S/S 3' was significantly greater than that of 'Grid S/S 1' and 'Grid S/S 3'. The power flow converged at Zero for all three 33kV sites at 80% of DG exposure.

The graphs indicate that power would flow upstream at all three 33kV sites at 100% exposure to DG. The rate of change in real power magnitude remained similar for all three sites despite the reversal of power flow, meaning most power flowing into the grid was through the 'Grid S/S 3' 33/132kV Tx.

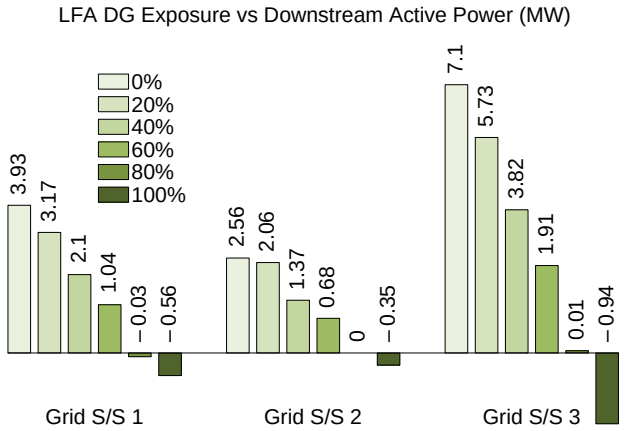

Fig. 3. LFA Model – LV DG exposure vs downstream active power from the grid.

When examining the graphs for summated power quantities, it can be said that the flow of real power is more affected than reactive power by the introduction of DG into the model. When

compared to the baseline, the summated real power being fed downstream from the grid moves to a further negative value with each increase in DG. The reactive power flowing through the grid sites moves to a more negative value than the baseline initially, but by Test 5 has swung to a greater value.

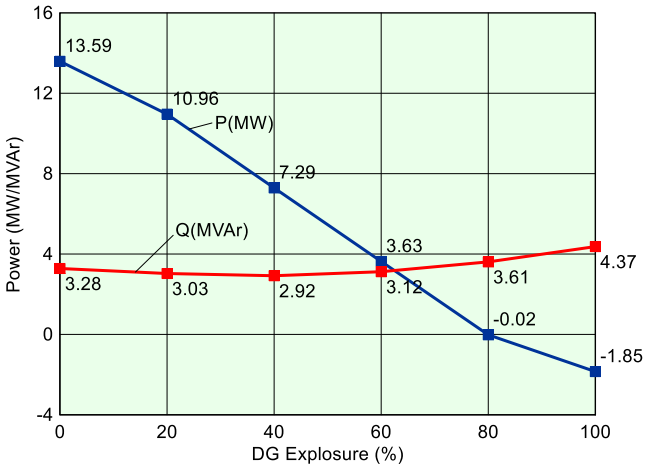

Fig. 4. LFA Model – Active power vs reactive power with increasing LV DG exposure.

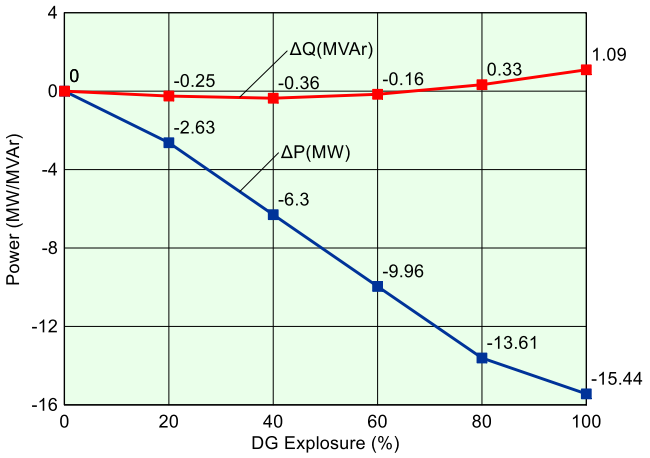

Fig. 5. LFA Model – Difference of active and reactive power vs baseline *PQ* values.

TABLE III. EXTRACT FROM PFA MODELLING RESULTS

Test No.#	DG (%)	Total 33kV Load Flow		Change in Load Flow *PQ*	
		***P* (MW)**	***Q* (MVAr)**	**Δ*P* from Baseline (MW)**	**Δ*Q* from Baseline (Mvar)**
1	0	13.59	3.28	0.00	0.00
2	20	10.96	3.03	-2.63	-0.25
3	40	7.29	2.92	-6.30	-0.36
4	60	3.63	3.12	-9.96	-0.16
5	80	-0.02	3.61	-13.61	0.33
6	100	-1.85	4.37	-15.44	1.09

From the data seen in Table III we can conclude that in the event that 14.8MW (80% in this model) or greater of LV connected renewable generation is feeding the distribution network, some of the active power in the network would reverse and flow upstream towards the grid. Protection against reverse power flow could be installed at each wind and solar farm. This would reduce the need for measures upstream but would rely heavily on the protection schemes remaining healthy and in service to work effectively in coordination [12].

VII. AUTOMATIC VOLTAGE CONTROLLER (AVC) DEVICES

On the SPM Network negative reactive compounding is used to control the mean average voltage output from a group of meshed 33kV substations and their associated 33/11kV transformers. It is used because, unlike on other UK networks, there is no direct connection between AVC's at different sites in the group; hence, substation A does not receive any information as to the tap state of the transformer at substation B or C. Typically, the NRC CT positioned on L2 of the LV side of the transformer along with a 3-phase VT input from the 11kV switchboard is used so that the AVC can derive power quantities. By knowing the reactive power magnitude and phase angle, the power factor can be derived and compared with a target PF. The AVC will tap the transformer (changing the primary voltage) when the load becomes less or more reactive in order to maintain a power factor that is close to the target [1].

VIII. FIELDWORK

An experiment was carried out to investigate the effects of reverse power flow on the AVC device when coupled with negative reactive compounding effects. The test involves ramping the phase angle of the yellow phase current until the power factor is moved far enough away from its target (0.985) to cause the AVC to attempt a tap. Under forward/downstream power flow conditions a current injection better than target PF causes the AVC to attempt to tap up by one tap; where a current injection worse than target PF causes the AVC to attempt to tap down by one tap.

To simulate real power flowing in the opposite direction (or abnormal/upstream load flow conditions), the CT input to the MicroTapp AVC was switched, and the experiment was repeated. When current connections I_b-I_n are reversed, the MicroTapp AVC displays the correct voltage, current, and power measurements. However, as expected, the angle of I_b is rotated 180 degrees. The AVC remains stable with the reverse connection whilst at target power factor, and it would tap correctly if the voltage magnitude determined by the 33/11kV transformer VT was out of the band.

Crucially, introducing compounding effects with the reverse connection in place causes the relay to attempt a tap in the wrong direction, and with the test held-on continues to issue this incorrect instruction.

IX. SOLUTION PROPOSAL

Improving the capacity of the network to absorb upcoming changes in supply and demand could take time and require significant infrastructure works. A simple but effective current input switching circuit could be integrated with existing wiring installations, where the yellow phase positive and neutral

secondary current wiring is switched depending on the direction of current flow through the 33/11kV transformer. The principle for this design is illustrated in Fig. 6.

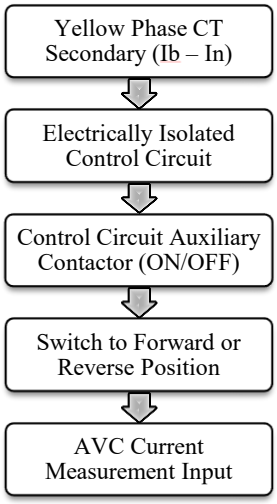

Fig. 6. AVC current input switching circuit process.

X. CONCLUSION

An inversion of CT input polarity to simulate upstream power flow would cause the AVC to issue an incorrect tap instruction when compounding effects are also present; in such a way that would cause a cascade of tapping operations which would continue to move the power factor further away from the target with each tap. In these circumstances, the 33/11kV transformer LV voltage would rapidly move further away from a suitable level for the network load profile.

Further study is needed to investigate the effects of EV uptake with the use of relevant year-by-year forecasting data that can be applied to the model for each test.

REFERENCES

[1] "Long term development statement." SP Energy Networks. https://www.spenergynetworks.co.uk/pages/long_term_development_statement.aspx (Accessed Dec. 11, 2019).

[2] "Government takes historic step towards net-zero with end of sale of new petrol and diesel cars by 2030." GOV.UK. https://www.gov.uk/government/news/government-takes-historic-step-towards-net-zero-with-end-of-sale-of-new-petrol-and-diesel-cars-by-2030 (Accessed Nov 18, 2020).

[3] E. Vugrin, and M. Baca, "Electric power system modelling and analysis," Sandia National Laboratories, May 2013. Accessed: Dec 08, 2020. [Online]. Available: https://www.osti.gov/servlets/purl/1083672

[4] A. Hooshyar, and R. Iravani, "Microgrid protection," *Proceedings of the IEEE*, vol. 105, no. 7, pp. 1332-1353, July 2017, doi: 10.1109/JPROC.2017.2669342

[5] Z. Jia, and B. Jeyasurya, "Contingency ranking for on-line voltage stability assessment," *IEEE Transactions on Power Systems*, vol. 15, no. 3, pp. 1093-1097, Aug. 2000, doi: 10.1109/59.871738

[6] M. Tajdinian, M. Allahbakhshi, M. Mohammadpourfard, B. Mohammadi, Y. Weng, and Z. Dong, "Probabilistic framework for transient stability contingency ranking of power grids with active distribution networks: application in post disturbance security assessment," *IET Generation, Transmission & Distribution*, vol. 14, no. 5, pp. 719-727, Mar. 2020, doi: 10.1049/iet-gtd.2019.0840

[7] J.-J. Deng, and H.-D. Chiang, "Convergence region of Newton iterative power flow method: Numerical studies," *Journal of Applied Mathematics*, vol. 2013, Art. no. 509496, 2013, doi: 10.1155/2013/509496

[8] G. Shrinivasan, *Power System Analysis*, 2nd ed. Pune, India: Technical Publications Pune, 2009.

[9] "SG 2.6-114 offshore wind turbine." Siemens Gamesa Renewable Energy. https://www.siemensgamesa.com/en-int/products-and-services/onshore/wind-turbine-sg-2-6-114 (Accessed Nov. 20, 2020).

[10] "Kilgallioch windfarm – Scottish Power renewables." Scottish Power Ltd. https://www.scottishpowerrenewables.com/pages/kilgallioch.aspx (Accessed Apr. 20, 2020).

[11] BRE, *Planning Guidance for the Development of Large Scale Ground Mounted Solar PV Systems*. Cornwall, UK: BRE National Solar Centre, 2013.

[12] K.N. Bangash, M.E.A. Farrag, and A.H. Osman, "Manage reverse power flow and fault current level in LV network with high penetration of small scale solar and wind power generation," in *Proc. 53rd Int. Universities Power Engineering Conference (UPEC)*, Glasgow, UK, 4-7 Sept. 2018, pp. 1-6, doi: 10.1109/UPEC.2018.8541923